

## Technical Report ARWSB-TR-09014

# Plasma Enhanced PVD Protective Coatings for Wear and Erosion

S.L. Lee, R. Wei, S. Smith, M. Todaro, E. Langa, K. Coulter, L. Collins, A. Welty

**April 2009**



ARMAMENT RESEARCH, DEVELOPMENT AND ENGINEERING CENTER  
Weapons & Software Engineering Center  
Benét Laboratories



Approved for public release; distribution is unlimited.

The views, opinions, and/or findings contained in this report are those of the author(s) and should not be construed as an official Department of the Army position, policy, or decision, unless so designated by other documentation.

The citation in this report of the names of commercial firms or commercially available products or services does not constitute official endorsement by or approval of the U.S. Government.

Destroy this report when no longer needed by any method that will prevent disclosure of its contents or reconstruction of the document. Do not return to the originator.

<b>REPORT DOCUMENTATION PAGE</b>				<i>Form Approved</i> <b>OMB No. 0704-0188</b>	
<small>Public reporting burden for this collection of information is estimated to average 1 hour per response, including the time for reviewing instructions, searching data sources, gathering and maintaining the data needed, and completing and reviewing the collection of information. Send comments regarding this burden estimate or any other aspect of this collection of information, including suggestions for reducing this burden to Washington Headquarters Service, Directorate for Information Operations and Reports, 1215 Jefferson Davis Highway, Suite 1204, Arlington, VA 22202-4302, and to the Office of Management and Budget, Paperwork Reduction Project (0704-0188) Washington, DC 20503.</small>					
<b>PLEASE DO NOT RETURN YOUR FORM TO THE ABOVE ADDRESS.</b>					
<b>1. REPORT DATE (DD-MM-YYYY)</b> 22/04/2009		<b>2. REPORT TYPE</b> Technical		<b>3. DATES COVERED (From - To)</b>	
<b>4. TITLE AND SUBTITLE</b> Plasma Enhanced PVD Protective Coatings for Wear and Erosion				<b>5a. CONTRACT NUMBER</b>	
				<b>5b. GRANT NUMBER</b>	
				<b>5c. PROGRAM ELEMENT NUMBER</b>	
<b>6. AUTHOR(S)</b> S.L. Lee, R. Wei, S. Smith, M. Todaro, E. Langa, K. Coulter, L. Collins, A. Welty				<b>5d. PROJECT NUMBER</b>	
				<b>5e. TASK NUMBER</b>	
				<b>5f. WORK UNIT NUMBER</b>	
<b>7. PERFORMING ORGANIZATION NAME(S) AND ADDRESS(ES)</b> U.S. Army ARDEC Benet Laboratories, RDAR-WSB Watervliet, NY 12189-4000				<b>8. PERFORMING ORGANIZATION REPORT NUMBER</b> ARWSB-TR-09014	
<b>9. SPONSORING/MONITORING AGENCY NAME(S) AND ADDRESS(ES)</b> U.S. Army ARDEC Benet Laboratories, RDAR-WSB Watervliet, NY 12189-4000				<b>10. SPONSOR/MONITOR'S ACRONYM(S)</b>	
				<b>11. SPONSORING/MONITORING AGENCY REPORT NUMBER</b>	
<b>12. DISTRIBUTION AVAILABILITY STATEMENT</b> Approved for public release; distribution is unlimited.					
<b>13. SUPPLEMENTARY NOTES</b>					
<b>14. ABSTRACT</b> Plasma enhanced magnetron technology utilizes an externally electron source to generate plasma in addition to conventional DC magnetron plasma. The technology was used to clean ASTM A723 steel surfaces prior to deposition, and to deposit adhesive coatings with improved properties. Ta coatings up to 286 µm were sputter deposited on flat and curved specimens cut from an A723 steel cylinder with 120mm diameter, with and without a sputtered Cr interface layer. It was shown that with enhanced surface cleaning prior to deposition and enhanced deposition with proper residual stress control, dense, adhesive, crack-resistant, pollution-free coatings can be deposited directly on A723 steel. Fractured surface of Ta showed excellent microvoid coalescence with ductile mode of fracture. Adhesion tests including groove test, cyclic pulsed laser heating test, and vented erosion simulator test demonstrated excellent adhesion, good structural and wear and erosion properties.					
<b>15. SUBJECT TERMS</b>					
<b>16. SECURITY CLASSIFICATION OF:</b>			<b>17. LIMITATION OF ABSTRACT</b> U	<b>18. NUMBER OF PAGES</b> 17	<b>19a. NAME OF RESPONSIBLE PERSON</b> Nicole Bentley
<b>a. REPORT</b> U/U	<b>b. ABSTRACT</b> U/U	<b>c. THIS PAGE</b> U/U			<b>19b. TELEPHONE NUMBER (Include area code)</b> 518-266-5606

## INSTRUCTIONS FOR COMPLETING SF 298

**1. REPORT DATE.** Full publication date, including day, month, if available. Must cite at least the year and be Year 2000 compliant, e.g., 30-06-1998; xx-08-1998; xx-xx-1998.

**2. REPORT TYPE.** State the type of report, such as final, technical, interim, memorandum, master's thesis, progress, quarterly, research, special, group study, etc.

**3. DATES COVERED.** Indicate the time during which the work was performed and the report was written, e.g., Jun 1997 - Jun 1998; 1-10 Jun 1996; May - Nov 1998; Nov 1998.

**4. TITLE.** Enter title and subtitle with volume number and part number, if applicable. On classified documents, enter the title classification in parentheses.

**5a. CONTRACT NUMBER.** Enter all contract numbers as they appear in the report, e.g. F33615-86-C-5169.

**5b. GRANT NUMBER.** Enter all grant numbers as they appear in the report, e.g. 1F665702D1257.

**5c. PROGRAM ELEMENT NUMBER.** Enter all program element numbers as they appear in the report, e.g. AFOSR-82-1234.

**5d. PROJECT NUMBER.** Enter all project numbers as they appear in the report, e.g. 1F665702D1257; ILIR.

**5e. TASK NUMBER.** Enter all task numbers as they appear in the report, e.g. 05; RF0330201; T4112.

**5f. WORK UNIT NUMBER.** Enter all work unit numbers as they appear in the report, e.g. 001; AFAPL30480105.

**6. AUTHOR(S).** Enter name(s) of person(s) responsible for writing the report, performing the research, or credited with the content of the report. The form of entry is the last name, first name, middle initial, and additional qualifiers separated by commas, e.g. Smith, Richard, Jr.

**7. PERFORMING ORGANIZATION NAME(S) AND ADDRESS(ES).** Self-explanatory.

**8. PERFORMING ORGANIZATION REPORT NUMBER.** Enter all unique alphanumeric report numbers assigned by the performing organization, e.g. BRL-1234; AFWL-TR-85-4017-Vol-21-PT-2.

**9. SPONSORING/MONITORS AGENCY NAME(S) AND ADDRESS(ES).** Enter the name and address of the organization(s) financially responsible for and monitoring the work.

**10. SPONSOR/MONITOR'S ACRONYM(S).** Enter, if available, e.g. BRL, ARDEC, NADC.

**11. SPONSOR/MONITOR'S REPORT NUMBER(S).** Enter report number as assigned by the sponsoring/ monitoring agency, if available, e.g. BRL-TR-829; -215.

**12. DISTRIBUTION/AVAILABILITY STATEMENT.** Use agency-mandated availability statements to indicate the public availability or distribution limitations of the report. If additional limitations/restrictions or special markings are indicated, follow agency authorization procedures, e.g. RD/FRD, PROPIN, ITAR, etc. Include copyright information.

**13. SUPPLEMENTARY NOTES.** Enter information not included elsewhere such as: prepared in cooperation with; translation of; report supersedes; old edition number, etc.

**14. ABSTRACT.** A brief (approximately 200 words) factual summary of the most significant information.

**15. SUBJECT TERMS.** Key words or phrases identifying major concepts in the report.

**16. SECURITY CLASSIFICATION.** Enter security classification in accordance with security classification regulations, e.g. U, C, S, etc. If this form contains classified information, stamp classification level on the top and bottom of this page.

**17. LIMITATION OF ABSTRACT.** This block must be completed to assign a distribution limitation to the abstract. Enter UU (Unclassified Unlimited) or SAR (Same as Report). An entry in this block is necessary if the abstract is to be limited.

## TABLE OF CONTENTS

Abstract .....	1
Introduction .....	1
Experimental Procedures .....	1
Surface Oxides on A723 Steel and Plasma Enhanced Ion Cleaning .....	2
Enhanced PVD Coatings Deposition and Characterization .....	3
Adhesion and Wear and Erosion Testing .....	3
Discussion .....	4
Conclusions .....	5
References .....	5

## LIST OF TABLES

Table 1: Experimental Conditions and Characterization of Ta and Ta/Cr depositions .....	7
---	---

## LIST OF FIGURES

Figure 1: Schematics of plasma enhanced magnetron system with filament generated plasma in additional to conventional DC magnetron plasma .....	8
Figure 2: Comparison of thin “native” oxide and thermal generated oxide on gun steel surfaces using AES analysis. The AES sputter rate is about 30nm/min .....	9
Figure 3: Cleanness study using SIMS analysis: ASTM A723 steel, heated in O <sup>18</sup> atmosphere for 3 hrs at 350°C to grow thick O <sup>18</sup> oxide layer in addition to native O <sup>16</sup> oxide layer. Top- Ta7, no cleaning; Bottom- Ta 11, after cleaning for 60 minutes, native or re-oxidized O <sup>16</sup> , and heat-generated O <sup>18</sup> oxides were removed .....	10

## LIST OF FIGURES (Continued)

Figure 4: Microstructure, Topography, Groove adhesion test for Ta and Ta on Cr depositions on steel: a- Ta3, b- Ta/Cr1, c- Ta/Cr5, d- Ta12-2, e- Ta13-15 microstructure, f- Ta12-2 groove test, g- Ta12-2 groove test, h- Ta13-15 groove test.....	11
Figure 5: XRD Phase Analysis of thick Ta depositions Ta13-15 and Ta13-20 on curved 120mm steel barrel section, showing bcc Ta with Ta (110) preferred orientation .....	12
Figure 6: Fractured surfaces of Ta13-15 on A723 steel- Fracture in substrate steel X1500 (left); Fracture in bcc Ta (right) showing microvoid coalescence with excellent ductile mode of fracture.....	13
Figure 7: Comparative Pulse Laser Heating test of sputtered Ta versus production electroplated Cr coatings- 10 cycles of laser pulses at 2.5 msec, 1.0 J/mm <sup>2</sup> simulating high bore temperature at ~1800°K, 80 μm Ta12-2 (top), 125μm Cr (1966-1) (bottom).....	14
Figure 8: Comparative VES (Vented Erosion Simulator) Firing Test- Ta 13-20 on gun steel after 129 high erosive rounds (top); electroplated HC Cr coated 120mm Cr1966-1 after 100 rounds (bottom), under the same simulated thermal-mechanical-chemical conditions as large cal firing .....	15

## ABSTRACT

Plasma enhanced magnetron technology utilizes an externally electron source to generate plasma in addition to conventional DC magnetron plasma. The technology was used to clean ASTM A723 steel surfaces prior to deposition, and to deposit adhesive coatings with improved properties. Ta coatings up to 286  $\mu\text{m}$  were sputter deposited on flat and curved specimens cut from an A723 steel cylinder with 120mm diameter, with and without a sputtered Cr interface layer. It was shown that with enhanced surface cleaning prior to deposition and enhanced deposition with proper residual stress control, dense, adhesive, crack-resistant, pollution-free coatings can be deposited directly on A723 steel. Fractured surface of Ta showed excellent microvoid coalescence with ductile mode of fracture. Adhesion tests including groove test, cyclic pulsed laser heating test, and vented erosion simulator test demonstrated excellent adhesion, good structural and wear and erosion properties. Plasma enhanced PVD technique, analytical and adhesion testing results, and applications of the technology for potential electroplated Cr replacement are discussed.

## INTRODUCTION

Transitional metals Cr and Ta have attractive properties to protective substrate steel against high temperature wear and erosion: High melting point temperature (Ta: 2996°C, Cr: 1857°C) compared to steel at 1535°C, chemical inertness, good ductility and formability, thermal and mechanical properties compatible with substrate steel. Ta is deposited in two phases: a softer and ductile stable *bcc*  $\alpha$ -phase, and a hard meta-stable *tetragonal*  $\beta$ -phase. Thick Ta coatings have been deposited on the interior surfaces of 120mm A723 steel cylinders using DC cylindrical magnetron sputtering systems [1-4]. Ta has also been deposited on a 20mm rifled tube using a triode sputtering system [5-6].

In a plasma enhanced DC magnetron system, external plasma is generated by an electron source, besides the conventional DC magnetron generated plasma [7-8]. The higher current density compared to conventional DC magnetron can more effectively clean up the substrate and to deposit quality coatings. A parametric investigation of Ta and Cr coating depositions using a planar magnetron sputtering system was reported [9]. A plasma enhanced cylindrical magnetron system has been constructed for deposition on the interior surface of a cylindrical structure [10]. Preliminary tests showed promising results, which will be reported in another paper. In this work, thick  $\alpha$ -Ta coatings up to 286  $\mu\text{m}$  were deposited on ASTM A723 steel with and without a sputtered Cr interface layer in an enhanced planar magnetron system and analytic and adhesion tests were performed.

## EXPERIMENTAL PROCEDURES

The schematic of a plasma enhanced magnetron system is shown in Figure 1. The filament generates independent global plasma in addition to the DC magnetron generated plasma. When electrons are generated from the filament source, they are accelerated to the chamber wall due to the positive potential. On the way to the wall, the electrons will experience collisions with the

neutral gas in the vacuum chamber such as Ar or Kr; and ionization occurs because of the high energy of the electrons ( $\sim 100\text{eV}$ ). As a result, plasma is generated. This electron-source generated plasma is independent of the magnetron-generated plasma. There are a number of advantages of this technique. First, during the substrate sputter-cleaning, the magnetrons do not need to be operated, while the electron-source generated plasma alone is sufficient to clean the substrate. In this way, deposition will not occur and cleaning is assured. Second, during the film deposition, the ion bombardment from the electron-source generated plasma is very intensive and the current density can be 25 times higher (current density at the substrate can increase from  $\sim 0.2\text{mA/cm}^2$  to  $\sim 4.9\text{mA/cm}^2$ ) than that with the magnetron-generated plasma alone. Third, the magnetron power can remain virtually unchanged. Consequently, a high ion-to-atom ratio can be achieved. The experimental conditions including cleaning and deposition parameters and characterization results are listed in Table 1: 1) Ta coatings on steel (Ta1-Ta5); 2) Ta on Cr on steel (Ta/Cr1-Ta/Cr5); 3) Thick Ta on steel (Ta12-2-Ta13-20). Note that sputter clean and deposition were carried out at 1.5-2.0 mTorr of Ar or Kr; Id is the discharge current used during the process, which is related to the plasma density; Vb and Ib are the sample holder bias voltage and the total current, respectively.

## **SURFACE OXIDES ON A723 STEEL AND PLASMA ENHANCED ION CLEANING**

A723 steel samples were cut into  $1'' \times 1/2'' \times 1/8''$  and mechanically polished using  $1\mu\text{m}$  diamond paste. Since ion cleaning to remove the surface oxide is of critical importance for coatings adhesion, a number of samples were purposely oxidized in a furnace at  $350^\circ\text{C}$  for 3 hours. This was to ensure a much thicker oxide layer than the native surface oxide formed on the surface. The comparison of the native oxide layer and the thermal oxide layer on A723 steel is shown in Fig. 2. The oxygen concentration depth profiles were taken using Auger Electron Spectroscopy (AES). Based on the AES analysis, thermal oxides are at least 20 times thicker than “native” oxides. Hence, it is believed that if the thermal oxides can be removed in sputter cleaning, it will be very safe to say that cleaning procedure is successful.

An innovative alternative technique for the cleanness study is to heat the steel samples at  $350^\circ\text{C}$  for 3 hours in  $\text{O}^{18}$  instead of  $\text{O}^{16}$  atmosphere, in order to differentiate it from native oxides residing on the steel surfaces. The oxidized samples were then ion sputter cleaned in Ar at Id = 10 Amp and Vb = 120 volts for 30, 60, 90 minutes; then sensitive Secondary Ion Mass Spectroscopy (SIMS) analysis was performed to obtain concentration depth profile. The data showed that ion cleaning for 60 minutes is sufficient to clean off all native and heat-generated oxides. In Fig. 3, SIMS data for Ta6 with no ion cleaning is shown in comparison with Ta 11 after 60 minutes cleaning.

## ENHANCED PVD COATINGS DEPOSITION AND CHARACTERIZATION

- a. In Table 1, cleaning and deposition conditions and characterization results for samples used in this investigation are listed. The Ta1-Ta4 samples were deposited at discharge current  $I_d = 10$  Amp. High compressive residual stresses from -2.9 to 1.0 GPa were observed on the film surface as the film grew thicker from 4 to 91  $\mu\text{m}$ , measured using X-Ray Diffraction. In thicker coatings, surface stress may appear low, but average stress is higher. Thus it is difficult to deposit thick films. To compare surface stress for two films of the same thickness: Ta2 deposited at  $I_d = 10$  Amp stress = -2.7 GPa, while Ta5 deposited at  $I_d = 0$  Amp stress = -1.5 GPa, both coatings were 10 $\mu\text{m}$  thick. This is expected since when the discharge current  $I_d$  is low, there are less ion bombardments, thus lower residual stresses. Hardness values stated in Table 1 were averaged throughout the thickness of the coatings. As the films grew thicker, hardness values decreased. Again, when hardness is compared for the same thickness film at 10 $\mu\text{m}$ : Ta2 deposited at  $I_d = 10$  Amp is almost twice as hard as Ta5 deposited at  $I_d = 0$  Amp. All Ta1-Ta5 samples showed dense and adhesive film morphology and bcc  $\alpha$ -Ta phase. In Fig. 4a, example Ta3 shows dense and adhesive microstructure.
- b. Crystalline lattice parameters of Cr are very close to those of steel; Cr may provide a bond layer for Ta deposition on steel. In Table 1, Ta/Cr1-Ta/Cr5 samples were deposited to see the effect of sputtered Cr interface layer of various thicknesses. Sputtered Cr appeared to be harder than Ta, but hardness in Ta is not affected by the thickness of interface Cr. In Figs. 4b and 4c, adhesion between Ta and Cr did not appear to be good, a line was observed, while Ta3 directly deposited directly on steel in Fig. 4a showed very good adhesion. The results suggested that sputtered Cr interface layer for Ta deposition may not be the best approach.
- c. The thick Ta12 series samples listed in Table 1 were deposited on flat polished steel samples; while thick Ta13-15 and Ta13-20 samples were deposited on curved samples cut from 120mm bore section. All Ta coating deposited in this section appeared dense, adhesive, with good topography and microstructure. In Fig. 4d, Ta 12-2 microstructure is shown. In Figs. 4e and 4f, Ta 13-15 topography and microstructure are shown. As stated, all Ta coatings in this investigation showed nearly 100% bcc Ta. In Fig. 5, XRD analysis of samples Ta13-15 and Ta13-20 showed that both samples were bcc  $\alpha$ -Ta with Ta (110) preferred orientation. In Fig. 6, fractured surface of substrate steel is compared with Ta coatings for sample Ta13-15. The sample was frozen in liquid nitrogen and then fractured. The dimples observed in the Ta fractured surface demonstrated excellent ductility, which is resilient to thermal shock cracking for high temperature wear and erosion gun barrel applications.

## ADHESION AND WEAR AND EROSION TESTING

ASTM B571-91 groove adhesion testing was used to test mechanical adhesion strength of thick coatings using a tungsten carbide tool. All thick coatings in Table 1 passed the groove adhesion test. Examples of groove test results are shown in Figs. 4g and 4h for samples Ta12-2 and

Ta13-15. Pulsed laser heating can test the thermal damages of coatings on a substrate under cyclic thermal pulses [11]. In Fig. 7, comparative pulsed laser heating test results performed for Ta12-2 and production electroplated Cr coatings are shown. Laser pulses at 2.5 msec, 1.0 J/mm<sup>2</sup>, 10 cycles were used to simulate the high temperature environment of large cal firing at ~1600°C. The 80 µm Ta12-2 sample shown on the top had no cracking, no delamination, and a thick HAZ (heat-affected-zone) in steel due to the smaller coatings thickness. The HAZ is due to the transformation of steel from tempered to untempered martensite. Thicker HAZ was observed due the relatively thin coating at 80µm. The 125µm electroplated Cr (1966-1) results are shown on the bottom, extensive cracks, HAZ, damages in Cr coatings and substrate steel were observed.

VES (Vented Erosion Simulator) has been used to simulate the thermal-mechanical-chemical environment of large cal firing using a steel fixture [1-2]. In Fig. 8, comparative VES testing results are shown for Ta13-20 on steel after 129 rounds of high erosive rounds on the top, and electroplated Cr after 100 rounds using the same simulated high erosive rounds on the bottom. There were no cracks, no delamination, no damages observed for Ta13-20. The HAZ was also very thin due to the thicker coatings. There were extensive damages in the coatings and substrate for the electroplated Cr sample, including as-deposited cracks, crack propagation, new crack growth, re-crystallization in Cr, and white and gray layers formed in steel due to erosion damages [12].

## DISCUSSION

Cr electroplating process has been used for decades for wear-corrosion-erosion protection for numerous industrial and military components. Electroplated Cr demonstrates excellent adhesion to steel. However, HC (high contraction) Cr has extensive as-deposited cracks; LC (low contraction) Cr has fewer but still has many cracks. The cracks will propagate and new cracks will grow. The cracks allow atmosphere or hot pressurized propellant gases (CO, CO<sub>2</sub>, H<sub>2</sub>, H<sub>2</sub>O, N<sub>2</sub>, NO, H<sub>2</sub>S etc.) to penetrate the coatings and interact with the substrate causing damages and failures in the coatings and substrate. Furthermore, Cr electroplating process generates toxic hexavalent Cr, detrimental to the environment and difficult and expensive to dispose. In this paper, we have shown a new plasma enhanced deposition process to deposit pollution-free, crack-resistant coatings, such as Ta, in planar geometry. The technology can be applied to coat industrial and military components, engine parts, gun barrels, cutting tools etc., for wear-erosion-corrosion applications, for potential electroplated Cr replacement.

Effective ion cleaning of substrate surface prior to deposition is critical to adhesion. The plasma enhanced cleaning process using argon ions demonstrated the removal of all surface oxides and debris to ensure adequate adhesion. Plasma enhanced deposition using biasing and increased current density can improve coatings quality, including structure, density, topography, and microstructure, with proper control of residual stresses. Residual stresses can cause cracking, buckling, and delamination. However, moderate compressive residual stresses on the coating surface in a tensile loading environment may be advantageous compared to tensile surface residual stresses. Plasma enhanced deposition process with proper choice of biasing voltage and

discharge current to control residual stresses demonstrated excellent VES (Vented Erosion Simulator) test results for high temperature wear and erosion applications.

## CONCLUSIONS

- a) Plasma enhanced PVD techniques using external plasma generated from a filament electron source demonstrated effective surface cleaning of all surface oxides and debris for improved adhesion.
- b) Plasma enhanced PVD deposition with proper control of residual stresses demonstrated the direct deposition of thick, dense, adhesive, bcc Ta coatings on A723 steel with excellent structure properties. A sputtered Cr interface layer is not necessary to enhance adhesion.
- c) Pulsed Laser Heating and Vented Erosion Simulator testing demonstrated excellent high temperature wear and erosion properties superior to electroplated Cr coatings under the same testing conditions.
- d) Plasma enhanced PVD process has good potential for Cr electroplating process replacement.

## REFERENCES

1. C.P. Mulligan, S.B. Smith, G.N. Vigilante, J. of Pressure Vessel Technology, 128, (2006) 240.
2. G.N. Vigilante and C.P. Mulligan, Materials and Manufacturing Processes 21 (2006) 621.
3. K. Truszkowska, M. Wotzak, F. Yee, G.N. Vigilante, M. Cipollo, SVC 47<sup>th</sup> Tech. Conf. Proc. (2004), 282.
4. F. Yee, M. Wotzak, M. Cipollo, K. Truszkowska, SVC 47<sup>th</sup> Tech. Conf. Proc. (2004) 421.
5. D.W. Matson, M.D. Merz, E.D. McClanahan, J. Vac. Science. Tech. A 10(4) (1992) 1791.
6. S.L. Lee, D. Windover, M. Audino, D.W. Matson, E.D. McClanahan, Surf. Coat. Tech. 149, (2002) 62.
7. J.N. Matossian, R. Wei, J. Vajo, G. Hunt, M. Gardos, G. Chambers, L. Soucy, D. Oliver, L. Jay, C. M. Taylor, G. Alderson, R. Komanduri and A. Perry, Surf. Coat. Tech., Vol. 108-109, (1998) 496.
8. R. Wei, J.J. Vajo, J.N. Matossian, and M.N. Gardos, Surf. Coat. Tech., Vol. 158-159 (2002) 465.
9. S.L. Lee and R. Wei, SVC 50<sup>th</sup> Tech. Conf. Proc. (2007) 441.

10. R. Wei and S.L. Lee, SVC 51<sup>st</sup> Tech. Conf. Proc. (2008) 559.
11. P. Cote, S.L. Lee, M. Todaro, G. Kendall, ASME J. of Pressure Vessel Tech. Vol. 125 (2003) 335.
12. P. Cote and C. Rickard, Wear 241 (2000), 17.

	Sputter Cleaning					Deposition						Characterization			
Sample No	Gas	Flow Rate (sccm)	Time (min)	Vb (V)	Id (A)	Ta/Cr Time (min)	Vb (V)	Ib (A)	Id (A)	Pm (kW)	Gas	Ta/Cr Thick (μm)	Surface Stress (GPa)	Ta/Cr Hard (HK10)	Steel Hard (HK10)
Ta-1	Ar	150	90	120	10	30	40	0.61	<b>10</b>	4	Ar	4	-2.9	1379	499
Ta-2	Ar	150	90	120	10	60	40	0.59	<b>10</b>	4	Ar	10	-2.7	1112	499
Ta-3	Ar	150	90	120	10	300	40	0.55	<b>10</b>	4	Ar	46	-2.3	1011	493
Ta-4	Ar	150	90	120	10	600	40	0.54	<b>10</b>	4	Ar	91	-1	602	481
Ta-5	Ar	150	90	120	10	60	40	0.17	<b>0</b>	4	Ar	10	-1.5	552	543
Ta/Cr1	Ar	150	90	120	10	60/5	40	0.17	<b>10</b>	4	Ar	11/0.66		518	442
Ta/Cr2	Ar	150	90	120	10	60/10	40	0.17	<b>10</b>	4	Ar	12/1.24		427	499
Ta/Cr3	Ar	150	90	120	10	60/20	40	0.17	<b>10</b>	4	Ar	13/2.5		514/736	499
Ta/Cr4	Ar	150	90	120	10	60/40	40	0.17	<b>10</b>	4	Ar	11/4.88		385	530
Ta/Cr5	Ar	150	90	120	10	60/80	40	0.17	<b>10</b>	4	Ar	19/9.6		598/574	563
														<b>(HK50)</b>	<b>(HK50)</b>
Ta12-2	Ar	150	90	120	10	300	40	0.87	<b>10</b>	4	Kr	80			
Ta12-5	Ar	150	90	120	10	600	40	1.06	<b>10</b>	4	Kr	100			
Ta12-7	Ar	150	90	120	10	840	40	1.06	<b>10</b>	4	Kr	177			
Ta13-15	Ar	150	120	120	10	900	40	1	<b>10</b>	4	Kr	161	-0.5	337	523
Ta13-20	Ar	150	+45	120	10	1200	40	1	<b>10</b>	4	Kr	286			

**Table 1: Experimental Conditions and Characterization of Ta and Ta/Cr depositions.**

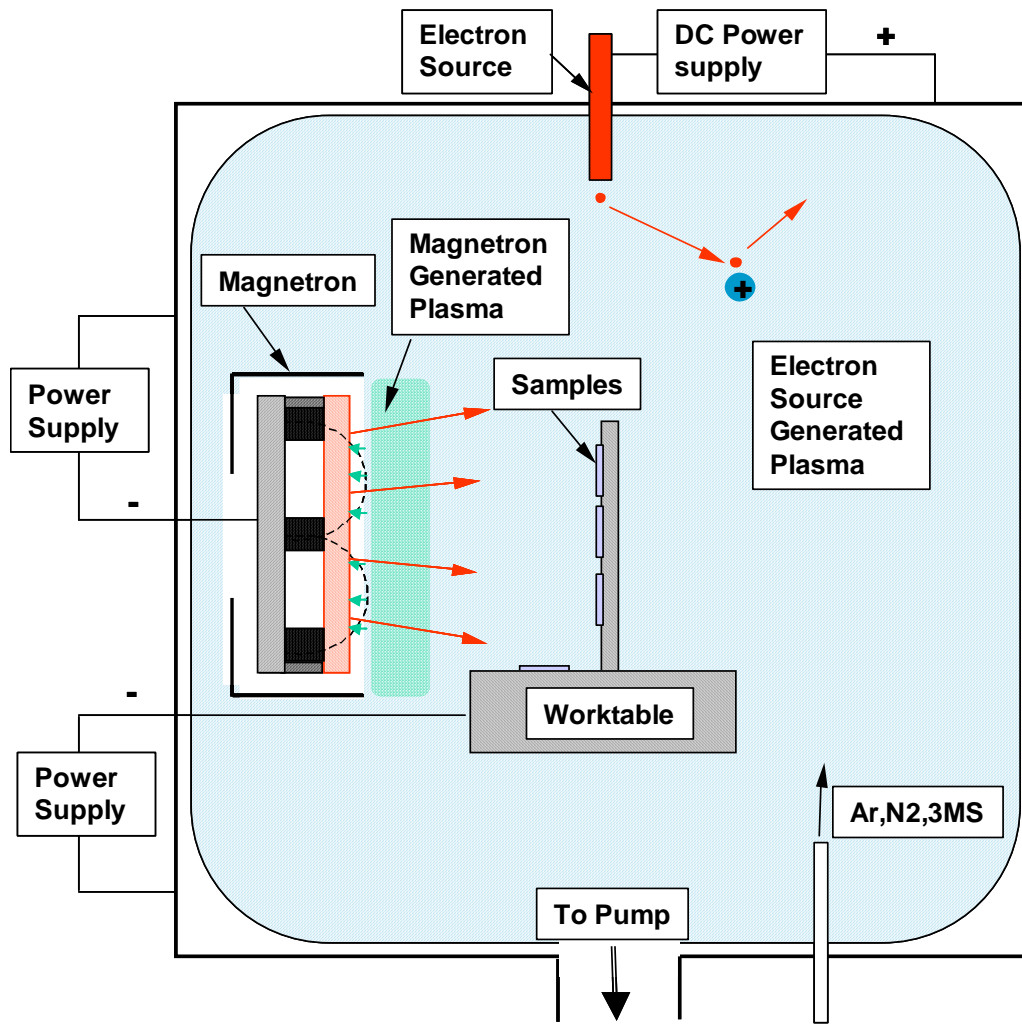


**Figure 1: Schematics of plasma enhanced magnetron system with filament generated plasma in addition to conventional DC magnetron plasma.**

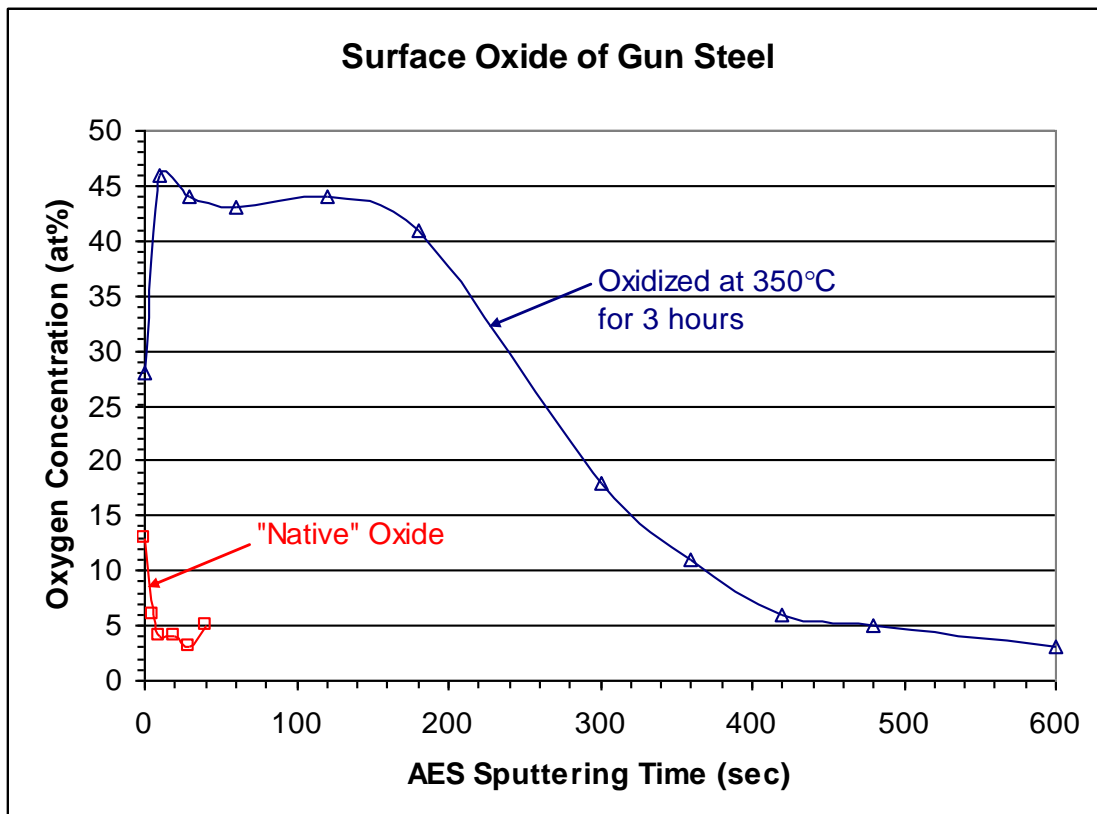


**Figure 2: Comparison of thin “native” oxide and thermal generated oxide on gun steel surfaces using AES analysis. The AES sputter rate is about 30nm/min.**

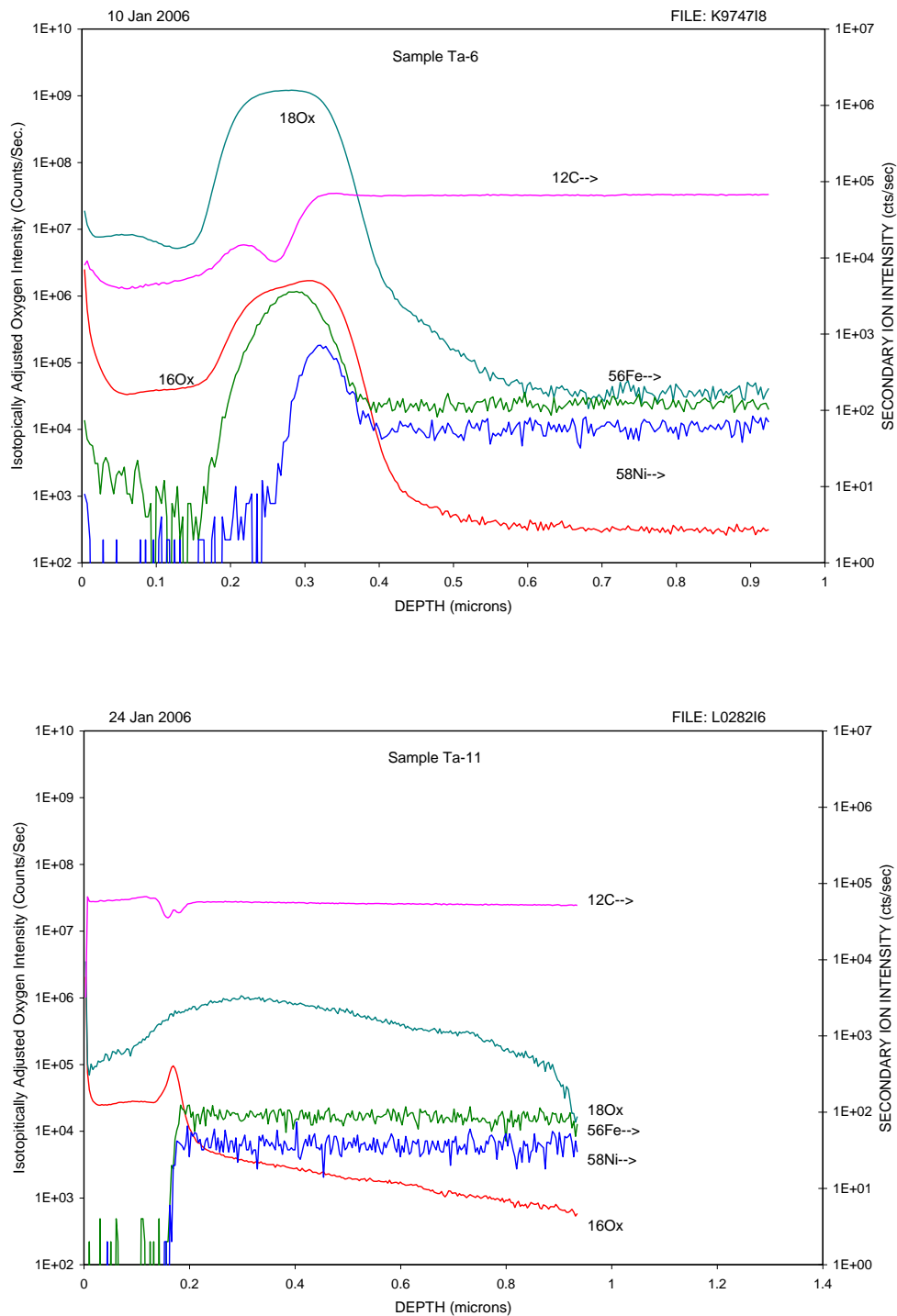


**Figure 3: Cleanness study using SIMS analysis: ASTM A723 steel, heated in  $O^{18}$  atmosphere for 3 hrs at 350°C to grow thick  $O^{18}$  oxide layer in addition to native  $O^{16}$  oxide layer. Top- Ta7, no cleaning; Bottom- Ta 11, after cleaning for 60 minutes, native or re-oxidized  $O^{16}$ , and heat-generated  $O^{18}$  oxides were removed.**

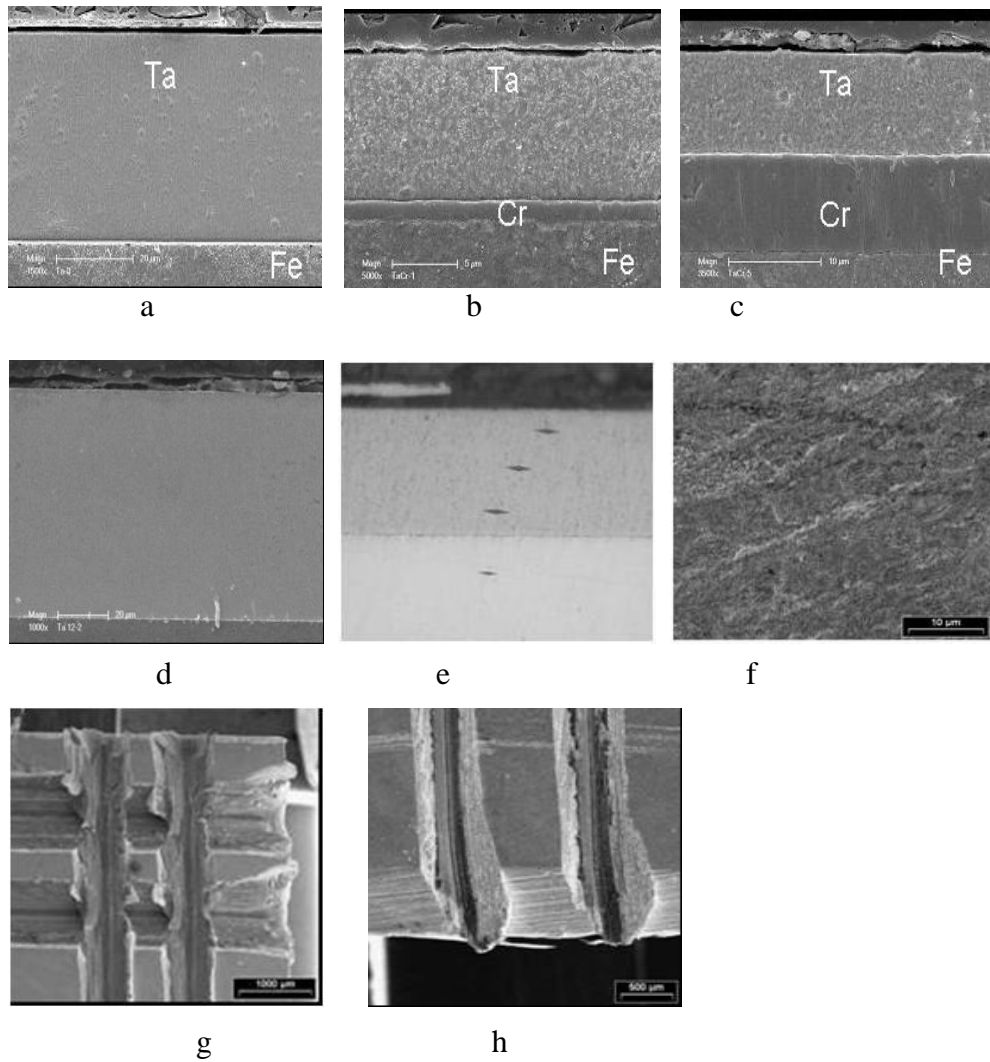


**Figure 4: Microstructure, Topography, Groove adhesion test for Ta and Ta on Cr depositions on steel: a- Ta3, b- Ta/Cr1, c- Ta/Cr5, d- Ta12-2, e- Ta13-15 microstructure, f- Ta12-2 groove test, g- Ta12-2 groove test, h- Ta13-15 groove test.**

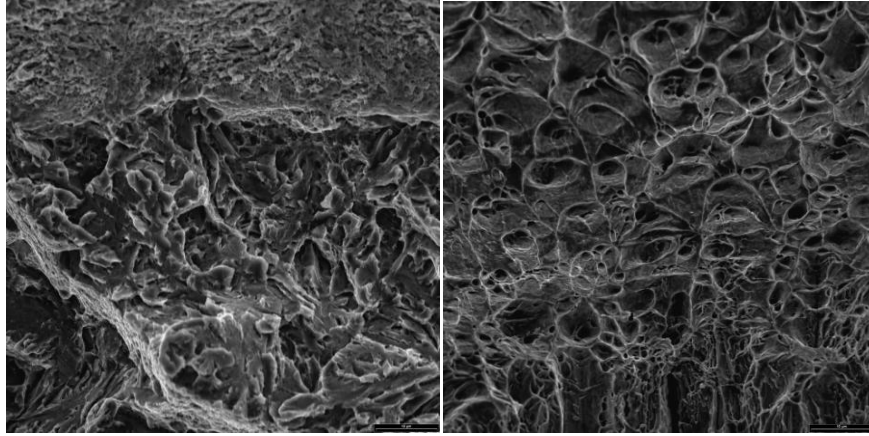


**Figure 5: XRD Phase Analysis of thick Ta depositions Ta13-15 and Ta13-20 on curved 120mm steel barrel section, showing bcc Ta with Ta (110) preferred orientation.**

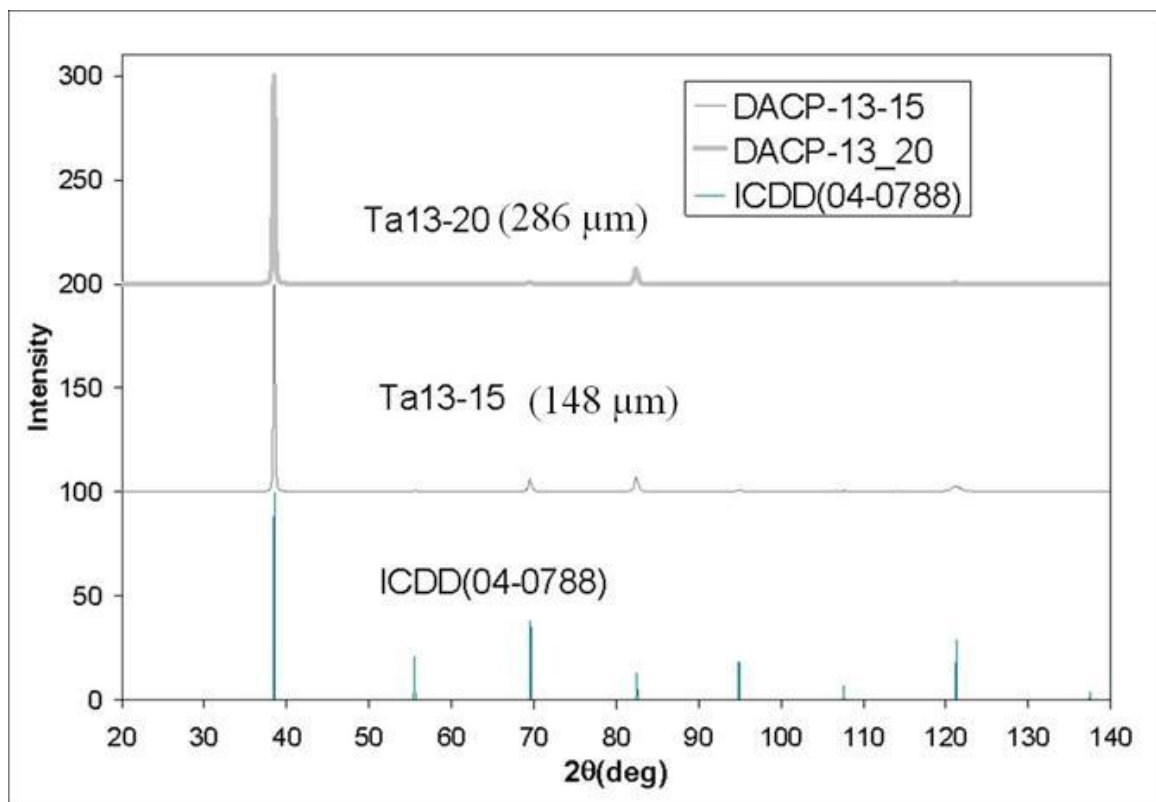


**Figure 6: Fractured surfaces of Ta13-15 on A723 steel- Fracture in substrate steel X1500 (left); Fracture in bcc Ta (right) showing microvoid coalescence with excellent ductile mode of fracture.**

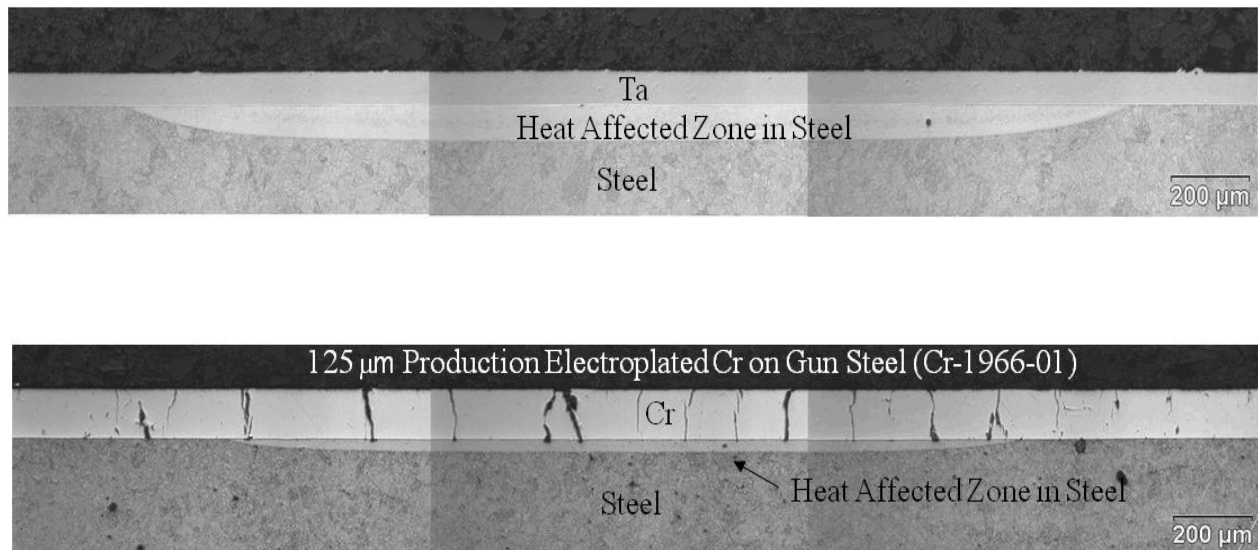


**Figure 7: Comparative Pulse Laser Heating test of sputtered Ta versus production electroplated Cr coatings- 10 cycles of laser pulses at 2.5 msec, 1.0 J/mm<sup>2</sup> simulating high bore temperature at ~1800°K, 80 μm Ta12-2 (top), 125μm Cr (1966-1) (bottom).**

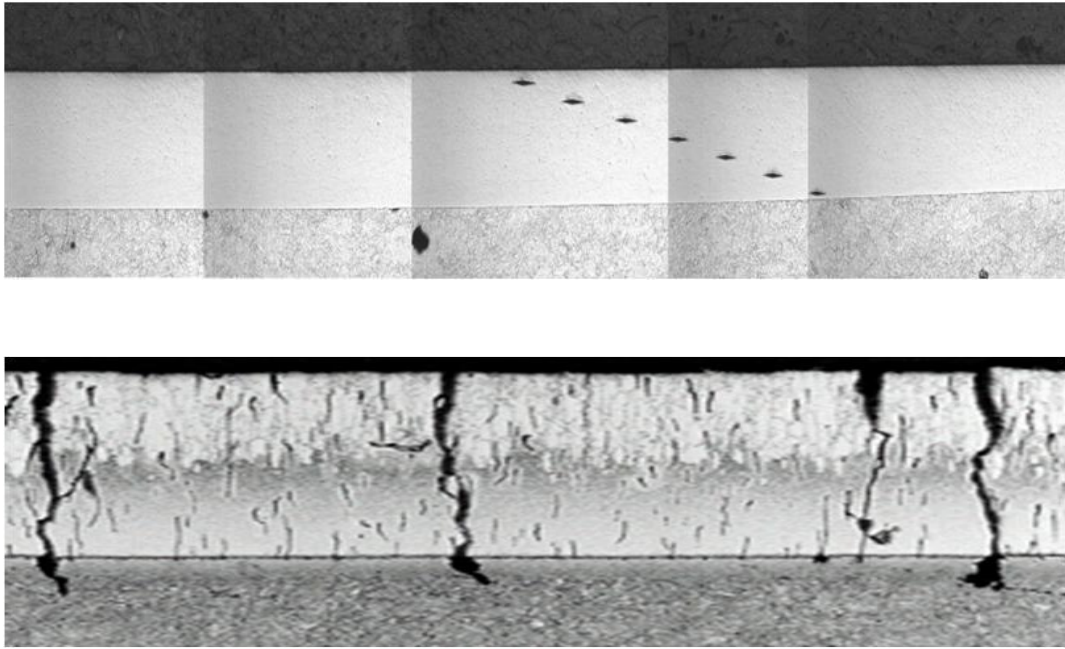


**Figure 8: Comparative VES (Vented Erosion Simulator) Firing Test- Ta 13-20 on gun steel after 129 high erosive rounds (top); electroplated HC Cr coated 120mm Cr1966-1 after 100 rounds (bottom), under the same simulated thermal-mechanical-chemical conditions as large cal firing.**